Anal. Chem. **2006,** *78,* 3234−3241

Articles

Magnetic and Gold-Coated Magnetic Nanoparticles as a DNA Sensor

Gilles K. Kouassi† and Joseph Irudayaraj*,‡

Department of Agricultural and Biological Engineering/Bindley Biosciences Center, The Pennsylvania State University, University Park, Pennsylvania 16802, and Department of Agricultural and Biological Engineering, Purdue University, 225 South University Street, West Lafayette, Indiana 47907

In this study, we report the chemical synthesis and functionalization of magnetic and gold-coated magnetic nanoparticles and the immobilization of single-stranded biotinylated oligonucleotides onto these particles. Selected sequences specific to the BRCA1 gene were used as a test platform. The binding of oligonucleotides to these particles was achieved through a streptavidin−biotin bridge via a carbodiimide activation protocol. Particle size and oligonucleotide attachment were confirmed by transmission electron microscopy; oligonucleotide binding was characterized by Fourier transform infrared spectroscopy and hybridization confirmed by fluorescence emission from the fluorophore attached to the target oligonucleotide strand. The rate of hybridization was measured using a spectrofluorometer and a microarray scanner. The rate of hybridization of oligonucleotides bound to the synthesized particles depends on the inorganic support material and its surface chemistry. The rate of hybridization increased concomitantly with the concentration of the probe and the target in the reaction medium. Furthermore, exposure of probe and target oligonucleotide to a combination of target and noncomplementary DNA strand reduced the rate of hybridization, possibly because of steric crowding in the reaction medium and cross-linking between reacting oligonucleotides and the noncomplementary strands. The study undertaken opens several possibilities in bioconjugate attachment to functionalized iron and iron nanocomposite structures for controlled manipulation and handling using magnetic fields.

The development of assemblies of inorganic materials with biomolecules has emerged as a novel approach to the controlled fabrication of functionalized nanostructures and networks. In the past two decades, the practice of DNA sequence detection has become more and more ubiquitous in genetics, pathology, criminology, food safety, and many other fields.[1] For example, single-strand DNA (ssDNA) probes immobilized to solid materials has proven to be a fundamental process in a variety of biotechnological[2] and biomedical applications,[3] including DNA-driven assembly of nanoparticles[1,4,5] and biosensors.[6] Furthermore, the hybridization of complementary DNA strands constitutes, either directly or indirectly, the basis for genome differentiation.[7] The choice of the support material is a central event in this process as it impacts the surface chemistry of the conjugation procedure and, more importantly, determines the practical use of the conjugates. Many platforms utilize solid-support inorganic materials tethered to DNA probes to capture single-stranded targets.[7]

To gain a comprehensive understanding of ssDNA immobilization and hybridization, evaluation of the kinetics is necessary so that quantification of the reaction is possible. Albeit abundant literature related to DNA hybridization exists, the number of studies addressing the kinetics of hybridization of oligonucleotides bound to nanosurfaces is limited. Furthermore, these studies are often carried out on 2-D assemblies. The rate of hybridization for surface-bound oligomers has been studied using the surface plasmon resonance,[3,8−10] surface plasmon diffraction,[11] and quartz crystal microbalance.[12] In recent years, a number of inorganic materials including various metal nanoparticles have been utilized to develop DNA array detection schemes because of the unique physical properties of these materials, including their large extinction and scattering coefficients, catalytic activity, surface electronic, and efficient Brownian motion in solution.[1] Gold nanoparticles have been reported as carrier materials for the

* Corresponding author. E-mail: Joseph Irudayaraj josephi@purdue.edu. Tel: (765) 494-0388. Fax: (765) 496-1115.

† The Pennsylvania State University.

‡ Purdue University.

(1) Fritzsche, W.; Taton, T. A. *Nanotechology* **2003**, *14*, 3194−3198.

(2) Sekar, M. M. A.; Bloch, W.; St. John, P. M. *Nucleic Acids Res.* **2005**, *33*, 366−375.

(3) Peterson, A. W.; Heaton, R. J.; Georgiadis, R. M. *Nucleic Acids Res.* **2001**, *29*, 5163−5168.

(4) Petrovikh, D.; Kimura-Suda, H. Whitman, L. J.; Tarlov, M. J. *J. Am. Chem. Soc.* **2003**, *125*, 5219−5226.

(5) Mir, K. U.; Southern, E. M. *Nat. Biotechnol.* **1999**, *17*, 788−792.

(6) Kerman, K.; Kobayashi, M.; Tamiya, E. *Meas. Sci. Technol.* **2004**, R1−R11.

(7) Riccelli, P. V.; Merante, F.; Leung, K. T.; Bortolin, S.; Zastawny, R. L.; Janeczko, R.; Benight, A. S. *Nucleic Acids Res.* **2001**, *29*, 996−1004.

(8) Fotin, A. V.; Drobyshev, A. L.; Proudnikov, D.; Perov, N. A.; Mirzabekov, A. D. *Nucleic Acids Res.* **1998**, *26*, 1515−1521.

(9) Georgiadis, R.; Peterlinz, K. P.; Peterson, A. W. *J. Am. Chem. Soc.* **2000**, *122*, 3166−3173.

(10) Nelson, B. P.; Grimsrud, E. T.; Liles, M. R.; Goodman, R. M.; Com, R. M. *Anal. Chem.* **2001**, *73*, 1−7.

(11) Yu, F.; Yao, D.; Knoll, W. *Nucleic Acids Res.* **2004**, *32*, e75.

(12) Okahata, Y.; Kawase, M.; Niikura, K.; Ohtake, F.; Furusawa, H.; Ebara, Y. *Anal. Chem.* **1998**, *70*, 1288−1296.

10.1021/ac051621j CCC: $33.50
Published on Web 04/20/2006

reverse aggregation of DNA,[13,14] and fabrication of DNA biosensor via the (3-mercaptopropyl)trymethoxysilane[15] protocol.

Magnetic nanoparticles as special biomolecule carriers via a suitable immobilization process offer promise as sensitive sensors. Magnetic nanoparticles have been used in immunoassays and in various reactions involving enzymes, proteins, and DNA for magnetically controlled transport and target delivery of anticancerous drugs.[16] Their reduced size and ability to be transported in biological systems and reacting medium is an advantage over conventional support systems. Gold and iron oxide-based magnetic nanoparticles (Fe_3O_4) seem to be the most desired nanoparticles because of their unique native properties. Considerable interest over the past two decades has been directed toward the functionalization of gold nanoparticles because of their excellent biocompatibility, stability, and established synthesis protocols. Furthermore, the use of thiol chemistry on a gold surface allows the attachment of molecules with a relative ease using a variety of thiol linkers.[14,17]

Magnetic nanoparticles owe their popularity to their numerous attributes such as their magnetic properties that enable them to be directed by an external magnetic field, the possibility to separate them from a reaction mixture, in addition to their low toxicity and biocompatibility. Hence, if the magnetic particles are provided with a gold coating, then the combined benefits of the robust chemistry for gold surfaces and the uniqueness of magnetic nanoparticles could be realized.[17−21] Recently, Fan et al.,[22] taking advantage of a magnetic separation/mixing process and the amplification feature of colloidal gold label, used gold-coated magnetic beads for immunoassay development. Hence, if DNA can be labeled with appropriate fluorophores, then their fluorescence quantum yields could be strongly enhanced upon hybridization, which can thus be imaged against a weakly fluorescing background.[22] It should be noted that although a considerable number of studies have been undertaken on the immobilization of DNA to nanoparticles, attention devoted to the kinetics of hybridization of oligonucleotides immobilized onto magnetic nanoparticles is still limited.

The present study reports the surface modification of magnetic nanoparticles, with amine group via silanization with (3-aminopropyl)trimethoxysilane (APTMS), the chemisorption of L-aspartic acid (LAA), and the carboxylation of gold-coated magnetic nanoparticle surfaces using mercaptoundecanoic acid. Subsequent functionalization of these particles using the biotin-modified DNA oligomer onto the magnetic nanoparticles was conducted by making use of the established biotin−streptavidin[23,24] bridge.[25] The kinetics of hybridization of the Quasar 670 fluorescent labeled target oligonucleotide was evaluated by fluorescence spectroscopy and the Genepix 4000A Microarray scanning measurements to assess the amount of bound target. The potential of the different surface chemistries and architectures is explored with respect to the segment of the BRCA1 gene as the target. The concentration of the probe and target was varied to improve the hybridization condition and to assess the assay specificity with respect to noncomplementary strands.

Table 1. Concentration of Streptavidin in the Supernatant after 1 h of Immobilization onto the Magnetic Nanoparticles (n =3)

	Fe_3O_4−APTMS	Fe_3O_4−LAA	Fe_3O_4@Au
streptavidin, nmol/mL	1.4 ± 0.2	0.4 ± 0.1	0.7 ± 0.1
binding efficiency, %	72	92	86

EXPERIMENTAL SECTION

Preparation of Magnetic Nanoparticles. Ferric chloride, 1-ethyl 3-(3-dimethylaminopropyl) carbodiimide hydrochloride (EDAC), sodium hydroxide, acetic anhydride, iron(II) chloride tetrahydrate 97%, iron(III) chloride hexahydrate 99%, nitric acid, (3-aminopropyl)trimethoxysilane, 1-butanol, octane, toluene, methanol, L-aspartic acid, tetramethylammonium bromide, 11-mercaptoundecanoic acid, and sodium tetrahydridoborate were obtained from Sigma-Aldrich (St. Louis, MO), and the NAP-10 columns were purchased from Amersham Biosciences (Newark, NJ). Genepix 4000A fluorescent microarray scanner from Axon Instruments (Union City, CA) and the spectrofluorometer (Packard Fluorocount, Packard Instrument Corp., Meriden, CT) were used for detection and binding confirmation. Oligonucleotides used in the present study include a capture sequence of the human breast cancer BRCA1 gene (Allain and Vo Dinh[26]), 5′biotin-d(spacer6-GAGCATACATAC)3′as the probe named ssDNA1, and its complementary Quasar 670 labeled sequence ssDNA-Quasar 670 (5′Quasar 670-d(spacer6-CTATGTATGCTC)3′. A second application involved the hybridization of a noncomplementary oligonucleotide from the genome of *Salmonella* Enteritidis denoted as ssDNA2 5′d(spacer6-CCAGACGACGACGAAAGA)3′ and its Quasar labeled counterpart, ssDNA2-Quasar 670 described as 5′Quasar670-d(spacer6-CCAGACGACGAAAGA)3′. Oligonucleotides were synthesized by Bioresearch Technologies Inc. (Novato). Streptavidin, a strain of *Streptomyces avidini* from Sigma was used to complete the streptavidin−biotin reaction. Buffers used in the experiment include the immobilization buffer (NaCl 300 mM, Na_2HPO_4 20 mM, EDTA 0.1 mM at pH 7.4) and the hybridization buffer (NaCl 150 mM, EDTA 0.1 mM at pH 7.4).

Preparation of Fe_3O_4 Magnetic Nanoparticles. Magnetic nanoparticles Fe_3O_4 were prepared by the hydrothermal coprecipitation of ferric and ferrous ions using NaOH as the base, described by Kouassi et al.[27] Typically iron(II) chloride and iron(III) chloride (1−2) were dissolved in Nanopure water at the concentration of 0.25 M iron ions and chemically precipitated at room temperature (25 °C) by adding 1 M NaOH at a constant of pH 10. The precipitates were heated at 80 °C for 35 min under continuous mixing and washed four times in water and several times in ethanol. During washing, the magnetic nanoparticles were separated from the supernatant using a magnetic separator of

(13) Hazarika, P.; Ceylan, B.; Niemeyer, C. M. *Angew. Chem. Int.* **2004**, *43*, 6469−6471.
(14) Minard-Basquin, C.; Kügler, R.; Matsuzawa, N. N.; Yasuda, A. *IEEE Proc-Nanobiotechnol*. **2005**, *152*, 797−103.
(15) Fu, Y.; Yuan, R.; Xu, L.; Chai, Y.; Zhong, X.; Tang, D. *Biochem. Eng. J.* **2005**, *23*, 37−44.
(16) Niemeyer, C. M. *Angew. Chem., Int. Ed.* **2001**, *4*, 4128−4148.
(17) Demers, L. M.; Mirkin, C. A.; Mucic, R. C.; Reynolds, R. A.; Leitsinger, R. L.; Viswanadham, G. A *Anal. Chem*. **2000**, *72*, 5535−5541.
(18) Zhou, W. L.; Carpenter, E. E.; Kumbhar, J. A. L.; Sims, J.; O'Connor C. J. *Eur. Phys. J*. **2001**, D *16*, 289−292.
(19) Lin, J.; Zhou, W.; Kumbhar, A.; Weimann, J.; Fang, J.; Carpenter, E. E.; O'Connor, C. J. *J. Solid State Chem*. **2001**, *159*, 26−31.
(20) Kim, K. D.; Mikhaylova, M.; Toprak, M.; Zhang, Y.; Bjelke, B.; Kehr, J.; Muhammed, M. *Mater. Res. Soc. Symp. Proc*. **2002**, *704*, W6.28.1.
(21) Mikhaylova, M.; Kim, K. D.; Berry, C. C.; Zogorodni, A.; Toprak, M.; Curtis, A. S. G.; Muhammed, M. *Chem. Mater*. **2004**, *16*, 2344−2354.
(22) Fan, A.; Lau, C.; Lu, J. *Anal. Chem*. **2005**, *77*, 3238−3242.
(23) Hards, A.; Zhou, C.; Seitz, M.; Bräuchle, C.; Zumbusch, A. *Phys. Chem*. **2005**, *6*, 534−540.
(24) Hamlett, K. J.; Kegley, B. B.; Hamlin, D. K.; Chyan, M.-K.; Hyre, D. E.; Press: O. W.; Wilbur, D. S.; Stayton, P. S. *Bioconjugate Chem*. **2002**, *13*, 588−598.
(25) Diamandis, E. P.; Christopoulos, T. K. *Clin. Chem.* **1999**, *37*, 625−636.
(26) Allain, L. R.; Vo-Dinh, T. *Anal. Chim. Acta* **2002**, *469*, 149−154.
(27) Kouassi, K. G.; Irudayaraj, J.; McCarthy G. *Biomagn. Res. Technol*. **2005**, *3*, 1.

strength greater than 20 megaoersted (MOe), and the particles were finally dried in a vacuum oven at 70 °C.

Surface Modification of Fe_3O_4 Magnetic Nanoparticles with APTMS. Magnetic nanoparticles (1 g) were washed with 99.5% methanol and twice with Nanopure water and soaked in 10 mL of 3 mM APTMS solution in a toluene/methanol (1:1 v/v) mix. The suspension was then transferred into a three-necked flask with a water-cooled condenser and temperature controller with a nitrogen gas flow at 80 °C for 20 h under vigorous stirring. Silanization was bound to occur at the surfaces of the particles bearing hydroxyl groups, which in the presence of an organic solvent results in the formation of an APTMS coating with a large density of amines.[20] The particles were recovered by applying an external magnetic field after the silanization process and washed three times with methanol and dried at 50 °C in a vacuum oven.

LAA Functionalization of Magnetic Nanoparticles. One gram of magnetic nanoparticles was immersed in 50 mL of 0.1 M LAA solution prepared in nitric acid at pH ~2. The mixture was sonicated for 15 min and vigorously stirred for 10 h at room temperature. An external magnetic field was applied to recover the particles and washed two times with Nanopure water. The process is expected to ensure the chemisorption of LAA, bearing carboxyl and amino groups on the surface of the particles.

Synthesis of Gold-Coated Magnetic Nanoparticles (Fe_3O_4@Au). The synthesis of gold-coated magnetic nanoparticles was accomplished using the method proposed by Lin et al.[19] Nanoparticles were prepared in a reverse micelle of cetyltrimethylammonium bromide (CTAB) using 1-butanol as a cosurfactant and octane as the oil phase. An aqueous mixture of ferric chloride hexahydrate and ferrous chloride tetrahydrate was then added to the prepared mixture. The size of the reverse micelle is dependent on the molar ratio of water to surfactant. The particles were prepared by choosing a molar ratio of water to CTAB, w as $[H_20]/[CTAB] = 8$. In brief, to 2.5 mL of solution A containing 1 M $FeCl_3$, 0.5 M $FeCl_2$, 6 g of CTAB, 5 g of butanol, and 15 g of octane was added 2.5 mL of a solution B containing 1 M $NaBH_4$ and the same composition of CTAB, butanol, and octane as in solution A. The blend was heated at 60 °C with vigorous mixing for 20 min to form magnetic nanoparticles. A 2-mL volume of solution C containing 0.44 M $HAuCl_4$, 3 g of CTAB, 2.5 g of butanol, and 1 g of octane, and an equivalent volume of solution D containing 1.6 M $NaBH_4$, 3 g of CTAB, 2.5 g of butanol, and 10 g of octane was successively added. The pH was kept at 11 by adding minute amounts of 0.5 M NaOH and continuously mixing for 15 min. The gold-coated magnetic nanoparticles were washed four times with water and several times with methanol and dried in a vacuum oven for 6 h.

Carboxylation of Gold-Coated Magnetic Nanoparticles Fe_3O_4@Au. Carboxylation of the gold-coated iron nanoparticles was done to allow the reaction of carboxyl groups on the surface of particles with the amino groups of streptavidin molecules after EDAC activation via an amide bond. Unfunctionalized magnetic nanoparticles (1 g) were added to a 10-mL ethanol solution of 20 mM 11-mercaptoundecanoic acid, sonicated for 48 h, and rinsed in Nanopure water. The surface of the particles was activated prior to covalent coupling by sonicating with 2 mL of EDAC (0.05 mg/mL) in water at 4 °C.

Immobilization of ssDNA onto the Functionalized Magnetic Nanoparticles. A 5-mg portion of Fe_3O_4−APTMS, Fe_3O_4−LAA, or Fe_3O_4@Au particles bearing amine and carboxylic groups was taken in a 50-mL polypropylene tube, 1 mL of EDAC (0.05 mg/mL) was added, and the mixture was sonicated for 25 min at 4 °C. The particles were separated using the external magnetic field of strength higher than 20 MOe and 5 nmol of streptavidin in a phosphate buffer solution. The mixtures were sonicated for 1 h, and the particles were then magnetically extracted from the supernatant. The Biorad Protein Assay reagent concentrate was used to determine the protein content of the supernatant using bovine serum albumin (BSA) as a protein standard. The absorbance was measured using the Beckman DU spectrophotometer at 505 nm, and the protein content was calculated using a standard curve made of known concentrations of BSA. The amount of streptavidin bound to the particles was then determined. A portion of biotin-labeled oligonucleotides (1−2-fold) in a stock solution, equivalent to the molar concentration of bound streptavidin, was added and incubated at room temperature for 2 h to allow the binding of biotinylated oligonucleotides to the streptavidin-coated magnetic nanoparticles.

Immobilization of Streptavidin. The immobilization of streptavidin onto the particle was evaluated by measuring the amount of streptavidin bound to the particles. In this assay, the protein content of the supernatant after the particles were separated using the magnetic separator was measured, using the Biorad Protein Assay reagent concentrate with BSA as the standard. The concentration of bound streptavidin was deduced from the concentration of streptavidin remaining in the supernatant after removal of the magnetic particles.

Hybridization Protocol. Hybridization was carried out at room temperature at 25 °C. Basically, equivalent concentration of the dye-labeled target oligonucleotide was added to the probe-tethered functionalized nanoparticles and the mixture (2 mL) was incubated for 4 h in the hybridization buffer. Selectivity of hybridization was assessed by incubating equal molar concentrations of noncomplementary strands simultaneously in the solution containing the probe and mixed thoroughly. Tubes were removed and vortexed at time intervals of 1 h for up to 4 h. Following mixing, 50-μL aliquots of the hybridizing solution were taken and the particles were separated from the supernatant and washed two times using the hybridization buffer. The hybridization buffer was added to the tube, and the fluorescent measurements were done for the DNA−particle complex. To compare the results of fluorescence measurement and to verify whether the presence of the particles affected the measurements, similar experiments were conducted and the bond formed between the immobilized DNA and the magnetic nanoparticles was destroyed by immersing the DNA−nanoparticle−fluorophore-labeled complex in 28% NH_4OH at 45 °C for 2 h with continuous shaking.[28] The magnetic nanoparticle conjugates were separated from the supernatant using the magnetic separator, and the duplex in solutions was purified using the NAP-10 column described by the manufacturer. Fluorescent measurements were then taken at 670 nm using a Packard FluoroCount spectrofluorometer in a filter wheel mode. For comparison purposes, the extent of hybridization was evaluated by measuring the fluorescence intensity of aliquots of the hybridization mixture as a function of time. The 3-μL aliquots of the hybridization mixture were taken and spotted on glass slides cleaned with ethanol beforehand. The fluorescence intensity of the spot was measured using the Genpix 4000A microarray scanner. Hybridization was confirmed by the fluorescence of the Quasar 670 labeled target oligonucleotide onto the probe-tethered particles. Fluorescence intensity of the spot was measured using the GenpixPro software. A standard curve was constructed by measuring the fluorescence intensity of the spots made of a known concentration of the Quasar 670-target oligonulceotide.

Hybridization Kinetics by Scanning Fluorescence and Spectrofluorometer. Hybridization of the ssDNA was assessed by (i) measuring the changes in the concentration of the target oligonucleotide using the spectrofluorometer and (ii) measuring

(28) Rivas, L.; Sanchez-Cortes, S.; García-Ramos, J. V.; Morrcillo, G. *Langmuir* **2000**, *16*, 9722−9728.

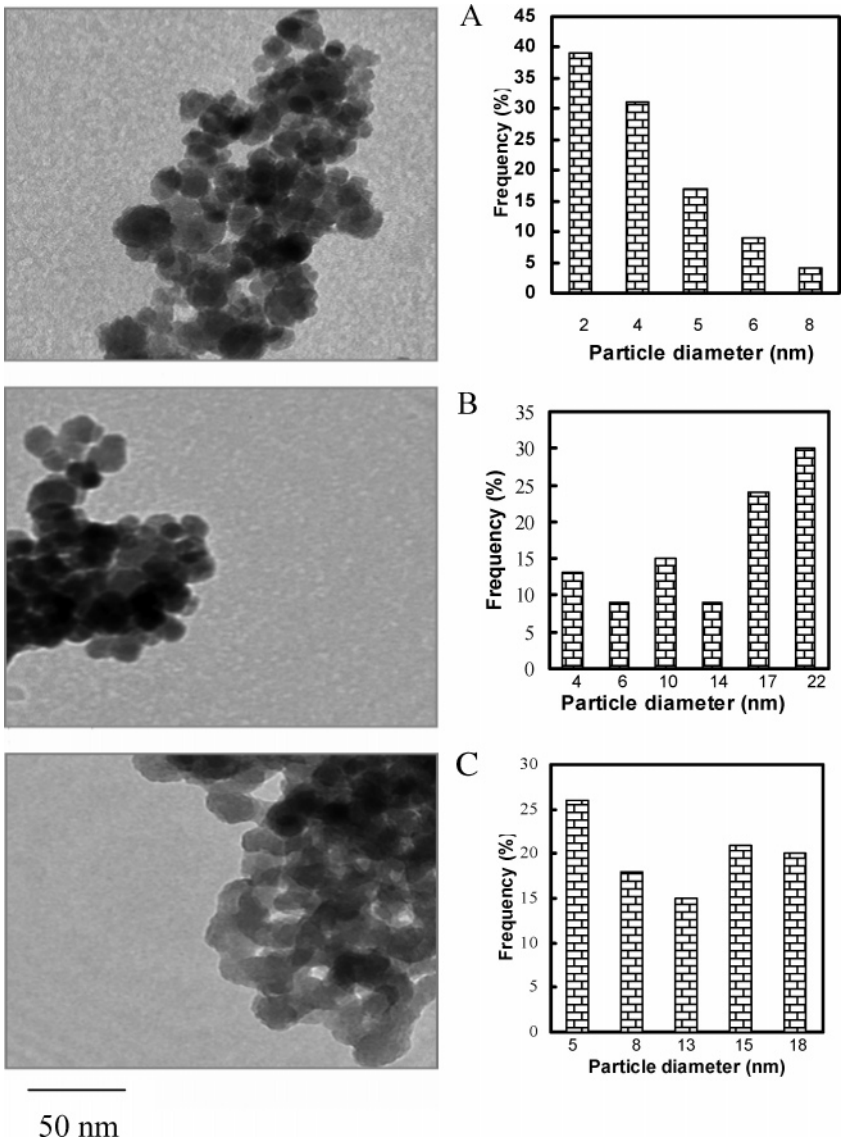

Figure 1. TEM images and particle size distribution of Fe_3O_4−APTMS (a), Fe_3O_4−LAA (b), and Fe_3O_4@Au (c) after the attachment of oligonucleotides.

the change in fluorescence intensity using the fluorometer (Genpix 4000A, Axon Instruments, Union City, CA.).

Characterization. To demonstrate the formation of the gold layer around the magnetic nanoparticles, gold colloidal and Fe_3O_4@Au solutions were prepared by dissolving 2 mg of $HAuCl_4$ and Fe_3O_4@Au, respectively, in 4 mL of water and the absorbance was measured using a UV−visible Beckman DU spectrophotometer. The size of magnetic nanoparticles were characterized by transmission electron microscopy (TEM, JEM 1200 EXII, Jeol) and presence confirmed by FT-IR spectroscopy (Biorad FTS 6000, Cambridge, MA). The samples for TEM analysis were prepared as follows: a drop of magnetic nanoparticles was dispersed in Nanopure water. The resulting solution was sonicated for 4 min to obtain better particle dispersion characteristics. A drop of the dispersed solution was then deposited onto a copper grid and dried overnight at room temperature. The binding of ssDNA onto the magnetic nanoparticles was confirmed using FT-IR spectroscopy. The media obtained after immobilization of ssDNA onto the magnetic nanoparticles were separated using a magnetic separator and washed with the immobilization buffer to remove the unbound oligonucleotides. The remaining ssDNA−magnetic nanoparticle conjugates were diluted in the immobilization buffer, and a drop of the mixture was deposited on the FT-IR sample holder for analysis.

Sensitivity Assay. To test the sensitivity of the bioconjugate complexes, different concentrations of the Quasar 670 labeled ssDNA varying from 10^{-7} to 10^{-5} nM were taken and the fluorescence intensity was measured using the spectrofluorometer and the microarray scanner. The DNA detection threshold values were determined following the analysis of the concentration-dependent values of fluorescent intensity to define the detected DNA concentration that yields a signal greater than three standard deviations above the background mean signal recorded without target.

Specificity Assay. The specificity of the bioconjugate complexes was tested by incubating ssDNA1 (5 nmol) immobilized onto Fe_3O_4−APTMS, Fe_3O_4−LAA, or Fe_3O_4@Au following the immobilization procedure described above with the noncomple-

(29) Penchovsky, R.; Birch-Hirschfeld, E.; McCaskill, J. S. *Nucleic Acids Res.* **2000**, *28*, 22e98.
(30) Velasco-Santos, C.; Martinez-Hernández, Lazada-Cassou, M.; Alvarez-Castillo, A.; Castaño, V. M. *Nanotechnology* **2002**, *13*, 495−498.

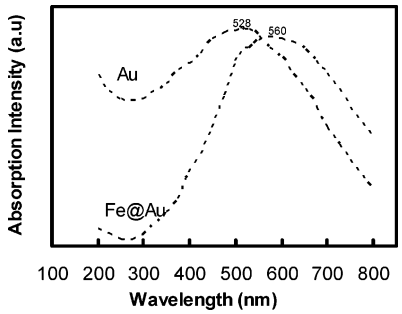

Figure 2. Absorption spectra of aqueous solutions of gold and Fe_3O_4@Au colloids measured using a UV−visible spectrophotometer.

mentary ssDNA 2-Quasar 670 for 2 h at room temperature. Aliquots of the samples (50 μL) were taken, and fluorescence measurements were recorded using the spectrofluorometer and the microarray scanner.

RESULTS AND DISCUSSION

Particles Size Distribution and Surface Chemistry. Synthesized iron particles have nearly a spherical shape and the size was between 4 and 8, 5 and 18, and 4 and 22 nm, respectively, for the Fe_3O_4−APTMS, Fe_3O_4−LAA, and Fe_3O_4@Au carboxyl-functionalized particles. The first two functionalized particles were made from Fe_3O_4 with an average size of 6 nm, prepared by coprecipitation of ferric or ferrous ions. It should be noted that the functionalization step tends to increase the particle size slightly. Consequently, Fe_3O_4−APTMS and Fe_3O_4−LAA were smaller than Fe_3O_4@Au particles. Fe_3O_4@Au nanoparticles functionalized with carboxylic groups (Fe_3O_4@AuCOOH) were slightly larger. This difference in size compared to the uncoated magnetic nanoparticles (Fe_3O_4−APTMS and Fe_3O_4−LAA) could have resulted from the gold shell (~3 nm thick) formed around the iron oxide core.

TEM images of the particles after DNA hybridization and particle size measurements of Fe_3O_4−APTMS, Fe_3O_4−LAA, and Fe_3O_4@Au are shown in Figure 1A−C, respectively. The Fe_3O_4−APTMS complex was prepared by silanization of magnetic nanoparticles with amino groups on the surface. Typically, APTMS, an organosilane coupling agent, has a silicon atom at the center of the molecule and contains an organic functional group along with methoxy or ethoxy groups. The inorganic groups of the molecule hydrolyze to silanol to form a metal hydroxide or siloxane bond with inorganic materials.[29] The surface modification of the magnetic nanoparticles with LAA is a chemical adsorption process in which the amino acid containing LAA is used as a chelating agent for the magnetic particles. Thus, intermediary molecules of the LAA can ensure complementary attachment of functional biomolecules.[22] After chemisorption, amino and carboxyl groups from the LAA were bound onto the surface of the magnetic nanoparticles, where the coupling between LAA and biomolecules could involve chemical bonds in the presence of a cross-linker.

The absorption spectrum of the colloid of Fe_3O_4@Au was measured and compared with that of a gold nanoparticle colloid prepared in the same way. The absorption band of the gold colloid has its maximum at 528 nm, while the Fe_3O_4@Au colloid shows a maximum at 560 nm (Figure 2). Results obtained were consistent with that reported by Lin et al.[19] and Rivas et al.[28] for the absorption maximum (526 nm) of pure gold colloid, while the absorption maximum for the Fe_3O_4@Au was consistent with the value

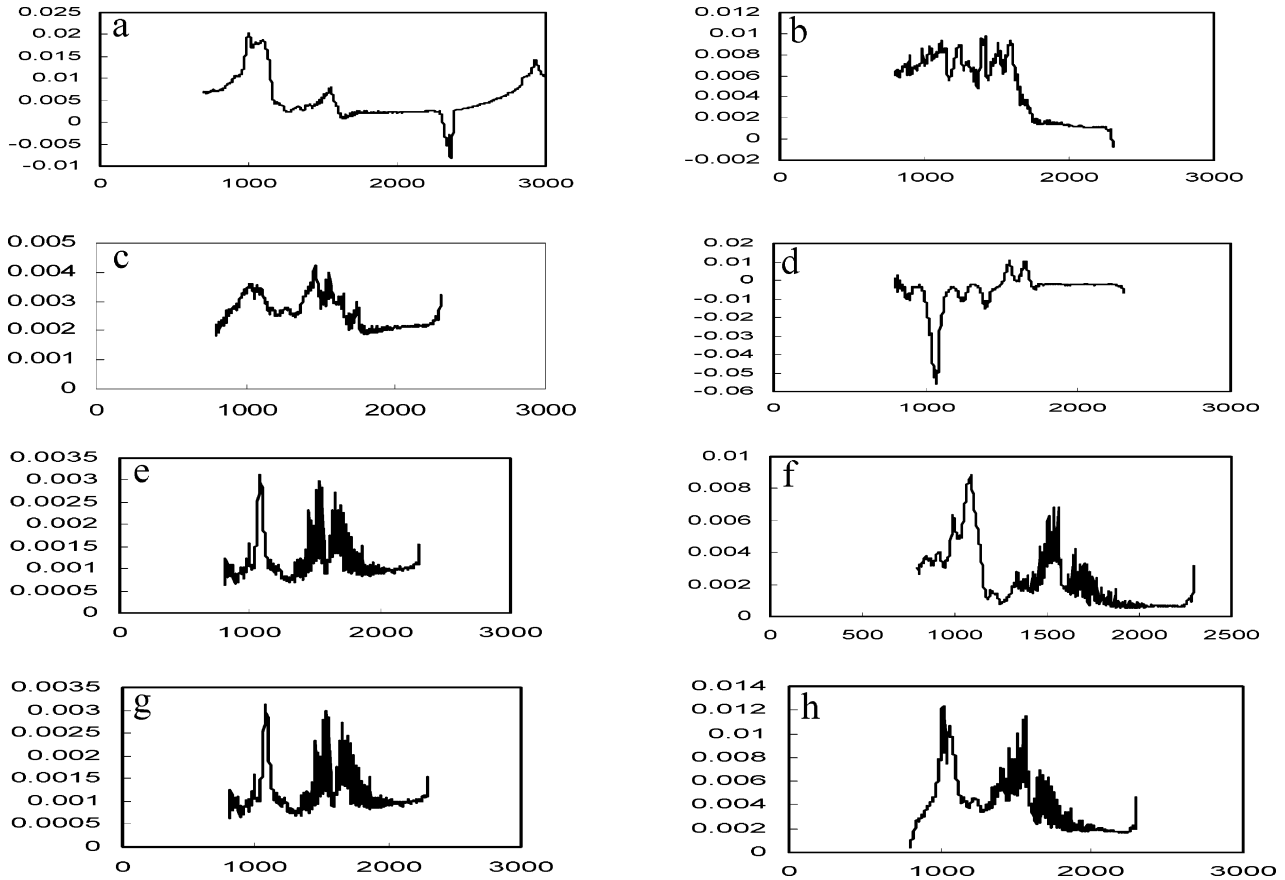

Figure 3. FT-IR spectra of Fe_3O_4−APTMS (a), Fe_3O_4−LAA (b), Fe_3O_4@Au (c), streptavidin (d), duplex ssDNA1−ssDNAQuasar670 (e), and Fe_3O_4−APTMS, Fe_3O_4−LAA, and Fe_3O_4@Au denoted respectively by (f), (g), and (h) after oligonuleotide immobilization.

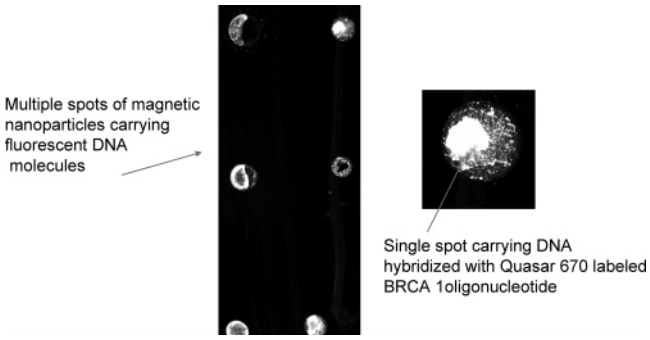

Figure 4. Fluorescence intensity image of the magnetic nanoparticle tethered spot conjugated with BRCA1−fluorophore complex on a glass slide using the microarray scanner.

reported by Lin et al.[19] The coupling of streptavidin to the three functionalized materials was initiated by the activation of the amino and carboxylate groups using carbodiimide. The binding of streptavidin to the particles after reacting with the functionalized particles activated with carbodiimide was estimated by measuring the amount of protein (streptavidin in the supernatant) after carbodiimide activation. Results of the measurements presented in Table 1 indicate that the binding efficiencies of streptavidin to the functionalized particles were 72, 92, and 86%, for Fe_3O_4−APTMS, Fe_3O_4−LAA, and Fe_3O_4@Au, respectively. A higher concentration of streptavidin was bound to Fe_3O_4−LAA since each molecule of LAA provided two binding sites including the amino and the carboxylic groups that are susceptible to binding to the protein after carbodiimide activation. On the contrary, each molecule of APTMS provided only a single binding site through its amino group. Similarly, a molecule of decanoic acid on Fe_3O_4@AuCOOH provides only a unique binding site through its carboxylic group. However, the effectiveness of Fe_3O_4@AuCOOH as a support for streptavidin immobilization is synonymous with a higher density of mercaptoundecanoic acid on the gold shell due to the affinity of the thiol chain to the gold surface.

FT-IR Results. The binding of oligonucleotide onto the particles was confirmed by FT-IR as shown in Figure 3. Spectra a−c, corresponding to Fe_3O_4−APTMS, Fe_3O_4−LAA, and Fe_3O_4@AuCOOH, respectively, depicted two sharp peaks in the region 1415−1300 cm^{-1} typical of carboxylate groups. Spectra a and b show prominent absorbance peaks at 1545 and 1635 cm^{-1} that are specific to amide I and amide II. These peaks confirmed the presence of amine groups on the surface of Fe_3O_4−APTMS and Fe_3O_4−LAA and the carboxyl groups provided through the attachment of mercaptobromoundecanoic acid on the surface of Fe_3O_4@Au. Spectra d−f depicted Fe_3O_4−APTMS, Fe_3O_4−LAA, and Fe_3O_4@Au bound to ssDNA1, hybridized with ssDNA1−Quasar 670. At 1720 cm^{-1}, in the spectrum (d−f) of ssDNA1, a perceptible peak assigned to carbonyl group in the thymine ring was noted. This peak is associated with a multitude of small peaks that enriched the spectra with features associated with various functional groups; hence, identification of peaks specific to carbonyl groups in the chemisorbed thymine ring was difficult. However, the presence of thymine on the surface of the particles confirmed the binding of oligonucleotide on these materials.

Immobilization and Hybridization. The immobilization of ssDNA was conducted by incubating the nanoparticle−streptavidin complex with the biotinylated ssDNA probes based on the well-known streptavidin−biotin noncovalent chemistry.[25] The binding efficiency of streptavidin to the biotinylated oligonucleotides presented in Table 1 was discussed earlier. Upon hybridization, the self-assembled duplex, the DNA−biotin−streptavidin conjugate was immobililized onto the magnetic nanoparticles. The duplex could then be removed from the reaction medium using an external magnetic field. The detection of fluorescence on the magnetic nanoparticles extracted after incubation of the immobilized probe with an equivalent amount of labeled target oligonucleotides after washing indicated that hybridization was effective. The fluorescence intensity on the surface of these particles could be used as a measure of the extent of hybridization measured using the spectrofluorometer and the microarray

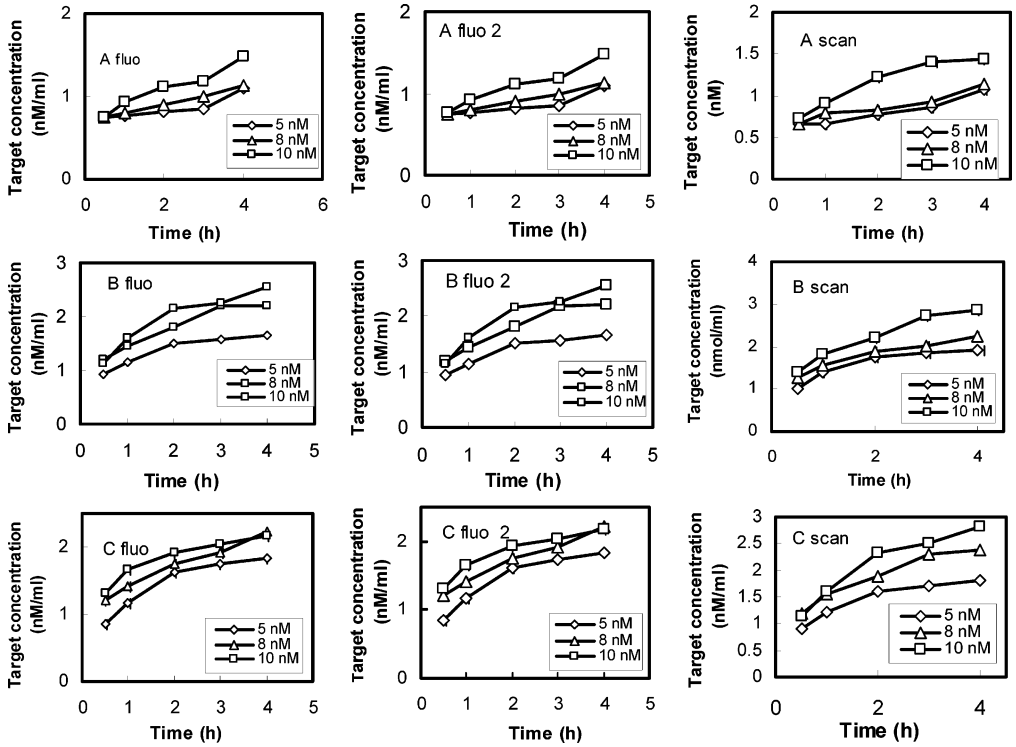

Figure 5. Kinetics of hybridization measured using a fluorescence spectroscopy before (A, B, C fluo), after the removal of magnetic nanoparticles (A, B, C fluo 2), and using a microarray scanner (A, B, C scan).

Table 2. Hybridization Rate Constants (h^{-1}) from the Second-Order Kinetics Model Measured from the Linear Regression Analysis of the Concentration of Fluorescent Target Oligonucleotide as a Function of Time[a]

target concn, nM	Fe_3O_4−APTMS	R^2	Fe_3O_4−LAA	R^2	Fe_3O_4@Au	R^2
5	0.1598 (sf)[b]	0.93	0.3396 (sf)	0.91	0.3259 (sf)	0.94
	0.1586 (sf)	0.95	**0.3386 (sf)**	0.97	**0.3221 (sf)**	0.90
	0.1353 (sm)[c]	0.89	0.3194 (sm)	0.97	0.3224 (sm)	0.89
8	0.1857 (sf)	0.98	0.3431 (sf)	0.93	0.3295 (sf)	0.95
	0.1860 (sf)	0.93	**0.3431 (sf)**	0.91	**0.3295 (sf)**	0.92
	0.1803 (sm)	0.95	0.3412 (sm)	0.89	0.3012 (sm)	0.93
10	0.3373 (sf)	0.88	0.6471 (sf)	0.90	0.6372 (sf)	0.88
	0.3376 (sf)	0.91	**0.6467 (sf)**	0.98	**0.6219 (sf)**	0.92
	0.3118 (sm)	0.99	0.6455 (sm)	0.96	0.6224 (sm)	0.95

[a] Values in boldface font represent the rate constants measured by spectrofluorometer after removal of particles from the duplex. [b] Hybridization measured by spectrofluorometer (sf). [c] Hybridization measured by scanner microaarray (sm).

scanner, for hybridization on Fe_3O_4−APTMS, Fe_3O_4−LAA, and Fe_3O_4@Au, respectively. Figure 4 shows examples of spots of hybridized DNA visualized using the microarray scanner. Results show a general increase in hybridization with time as the concentration of probe and target increased. However, the rate of hybridization was different from one support system to another. The lowest rate of hybridization was obtained with the Fe_3O_4−APTMS conjugate, while the highest was achieved with the Fe_3O_4−LAA support system assessed by spectrofluorometric measurements obtained before Figure 5 (A−C fluo) and after Figure 5 (A−C fluo 2) following removal of particles from the duplex. It can thus be deduced from the closeness of the data obtained from the hybridization kinetics described above that the hybridization profile was the same irrespective of the presence or absence of the particles. Basically, hybridization increased linearly as the concentration of target oligonucleotides increased, and the highest rate of hybridization was observed with the Fe_3O_4−LAA complex, where the concentration of the target was nearly twice. The second highest was the Fe_3O_4@Au system, where the extent of increase was ~1.7-fold, for measurements taken from 0.5 to 4 h. Results obtained from hybridization measured using the microarray scanner in Figure 5 (A−C scan) show a similar trend and confirmed the validity of the experimental procedure. Examples of hybridization rate constants measured with the spectrofluorometer at three distinct target densities (5, 8, and 10 nm) presented in Table 2 were 0.3396, 0.3431, and 0.6471; 0.3259, 0.3295, and 0.6372; and 0.1598, 0.1857, and 0.3373 h^{-1} for Fe_3O_4−LAA, Fe_3O_4@Au, and Fe_3O_4−APTMS, complexes, respectively. These results indicated that the rate of hybridization increased by increasing the concentration of target, and the rate of hybridization was different from one complex to another. Data obtained from the fluorometric detection of ssDNA1−Quasar 670 target using fluorescence spectroscopy before and after the removal of particles (Figure 5) were very similar and quantitatively comparable to the curves from the hybridization rate measured using the microarray scanner presented in Figure 5 (A−C scan). The concomitant increase in the rate of hybridization with the concentration of oligonucleotide shows that the concentration of probe and target is a determining factor in the assessment of hybridization. The extent of hybridization achieved on each magnetic support is consistent with the extent of streptavidin immobilized onto the support material. The overall rate constants of hybridization calculated from both fluorescence intensity measurement methods are shown in Table 2.

Sensitivity Assay. A sensitivity assay is an essential requirement for a viable DNA hybridization approach. Sensitivity is defined here as the minimum amount of target (analyte) DNA that can be reproducibly detected based on the ratio of analyte signal to that recorded for the background. The limit of detection is defined as the minimum concentration that yields a signal three standard deviations above the blank concentration and is determined to be 10^{-6} and 10^{-7} nM for measurements done using the fluorescence spectroscopy and the microarray scanner, respectively. Figure 6 (a and b) shows the sensitivity assay depicted by the concentration versus the fluorescence intensity plot for the spectrofluorometer and the microarray scanner, respectively. Results indicate that the microarray scanner is a very good candidate for hybridization assessment.

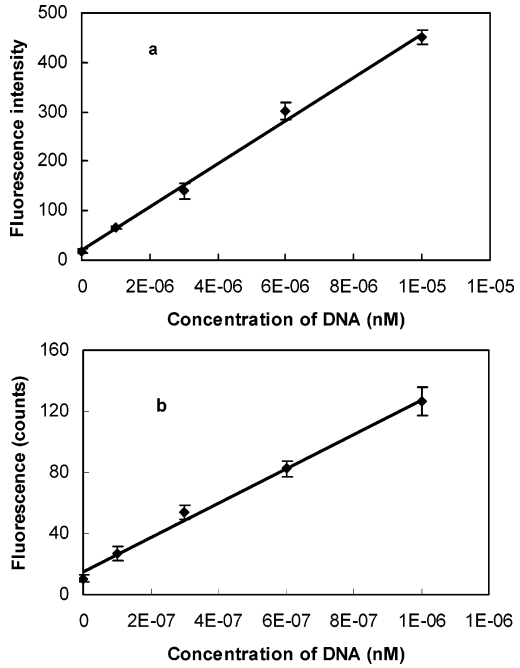

Figure 6. Sensitivity assay of ssDNA1−Quasar 670 detection using the spectrofluometer (a) and the microarray scanner (b). The fluorescence emission intensity of aliquots in solution and spots on glass slides as measured by the spectrophotometer and the microarray scanner, respectively, and plotted with respect to concentration.

Selectivity Assay. No measurable fluorescence intensity was found from the fluorescence spectroscopy measurement, and no fluorescence signal was detected from measurements carried out with the microarray scanner after exposure of ssDNA1 to the noncomplementary oligonucleotide ssDNA2−Quasar 670, indicating that hybridization did not occur. The failure of hybridization

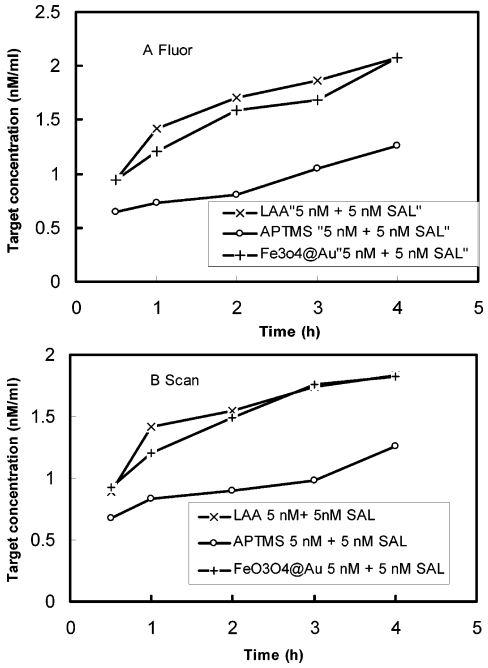

Figure 7. Hybridization kinetics measured at a fixed probe and target concentration in the presence of noncomplementary strands of *Salmonella enteritidis* (SAL), using the spectrofluorometer (A Fluor) and the microarray scanner (B Scan). 50 nm.

between ssDNA1 and ssDNA2−Quasar 670 compared to the effective hybridization of ssDNA1 with the complementary ssDNA1−Quasar 670 confirmed the capability of the bioconjugate systems to discriminate between a target and a noncomplementary strand, effectively. Hybridization of ssDNA1 on Fe_3O_4−APTMS, Fe_3O_4−LAA, and Fe_3O_4@Au support with its Quasar 670 counterpart was monitored after adding an equimolar amount of ssDNA2, to estimate the effect of noncomplementary oligonucleotide on the rate of hybridization. Figure 7 (a and b) depicts the extent of hybridization of ssDNA1 and complementary ssDNA1−Quasar 670 as a function of time. The trend in Figure 7a (data from spectrofluorometer) and Figure 7b (data from microarray scanner) was similar, indicating an increase in hybridization. The extent of rate increase was different from one support to another, in the order of Fe_3O_4−APTMS, Fe_3O_4@Au, and Fe_3O_4−LAA. Furthermore, the rate constants measured using the microarray scanner at a fixed target density of 5 nM, 0.1481, 0.2883, and 0.2777 on Fe_3O_4−APTMS, Fe_3O_4−LAA, and Fe_3O_4@Au, support, respectively (Table 2), were lower than that obtained when the hybridization mixture was devoid of ssDNA2. The extent of reduction was evaluated to be ∼9%. Since oligonucleotide capture did not take place when ssDNA1 was exposed to ssDNA2, the relative low hybridization rate may reflect the low accessibility to incoming hybridizing strands on the highly loaded nanoparticles, due to a combination of steric congestion of the bases and electrorepulsive interactions between the hybridizing strands and the noncomplementary oligomers. The proof of selectivity observed in our work confirms the viability of the bioconjugates and their effectiveness of our detection assay.

CONCLUSIONS

We have shown that single strands of oligonucleotides can be immobilized onto amino- and carboxylate-functionalized magnetic as well as gold-coated magnetic nanoparticles using the streptavidin−biotin interaction, after carbodiimide activation. The immobilization of streptavidin was more effective when the particles were functionalized by L-aspartic acid because of the availability of two binding sites through its carboxyl and amino groups. We have also demonstrated that DNA hybridization can be directly quantified using the microarray scanner. This study demonstrates that the rate of hybridization was related to the extent of bound streptavidin to the particles, and gold-coated magnetic nanoparticles are ideal DNA sensors. The rate of hybridization increased as the density of probe and target increased, but the presence of noncomplementary DNA sequence reduced the rate of hybridization probably due to steric crowding of the surface by the particles. The success of immobilization and hybridization on these organic surfaces and the information generated on kinetics of hybridization is a valuable step in the assessment of assay sensitivity and specificity.

Received for review September 10, 2005. Accepted March 22, 2006.

AC051621J